ADVANCED MATERIALS

temperature. A drastic reduction of the PL efficiency and a change in the vibrational structure of the PL spectrum were effected by MWNTs. The reduction of the PL efficiency can be a result of energy transfer and partial hole transfer from PPV chains to MWNTs, together with scattering and absorption by MWNTs. Using the composite, photovoltaic devices have been fabricated by employing MWNT as a hole-collecting electrode. We obtained good quantum efficiency (1.8 % at 2.9–3.2 eV), about twice that of the standard ITO device. It is considered that the high efficiency arises from a complex interpenetrating network of PPV chains with MWNTs and the relatively high work function of the MWNT film. The present results suggest the possible application of carbon nanotubes as a new interesting electrode material in macroscale devices.

## *Experimental*

The MWNTs were synthesized by the catalytic pyrolysis of hydrocarbons in the presence of a transition metal [20]. These catalytically grown MWNTs are essentially free from carbon impurities, such as tetrahedral carbons, fullerenes, and nanoparticles. Although they suffer from a greater concentration of structural defects than arc-evaporated MWNTs and, thus, are not perfect one-dimensional conductors, they are suitable for the present study because their nanoscale diameter allows the production of nanoscopically mixed composites. In order to obtain a concentrated dispersion of MWNTs, the raw MWNT sample was oxidized in acid solution ($HNO_3$ and $H_2SO_4$ mixed 1:3) for 2 h and then filtered and washed thoroughly with distilled water. After the oxidation, no traces of catalytic metals were observed by X-ray microanalysis [11] and X-ray photoelectron spectroscopy (XPS) [16] measurements. The surface groups generated by this treatment, such as carboxyl and alkoxyl groups, form a hydrophilic surface on the MWNTs and stabilize dispersions in water without surfactant. Details of the structure of these MWNTs as well as the oxidation method are reported elsewhere [11].

Thin films of MWNT were spin-coated onto a glass or quartz substrate from dispersions with concentrations of 0.5–2.0 wt.-%. The thickness of films can be controlled (from 20 to 300 nm) by altering the concentration or the spinning speed. For PL measurements and photovoltaic devices, we spin-coated the PPV precursor (sulfonium salt) onto MWNT films, ITO, or quartz, followed by thermal conversion at 210 °C for 10 h in vacuum [4]. This heat treatment stimulates the penetration of PPV into the MWNT layer and forms a good composite as described below. Finally, semi-transparent Al (with a transparency of about 40 % in the absorption range of PPV) was evaporated on top of the PPV layer to act as a second contact for the photovoltaic devices. Since the light was shone through the Al electrode during the photovoltaic measurements, we evaporated Al from the same batches for both MWNT/PPV/Al and ITO/PPV/Al devices to ensure the validity of any comparisons.

Film thickness was measured with a Dektak IIA profilometer. The morphology of MWNT and PPV–MWNT films was investigated by FE-SEM using a JEOL JSM-6340F operating at 10 keV. In order to study the morphology, we mechanically cleaved the composite with a microtome after encapsulation in epoxy resin. AFM was also applied to the surface of a MWNT film to investigate the depth profile using a Nanoscope IIIa.

The absolute PL efficiency was obtained using an integrated sphere connected to an Oriel Instaspec IV spectrophotometer through a liquid light guide. The 458 nm line of an Ar ion laser was used as an excitation source. The device characteristics were evaluated with a Keithley 237 source-measure unit under a vacuum of $10^{-5}$ torr. The device was illuminated through a semi-transparent Al electrode using a tungsten halogen lamp dispersed by a Bentham M300 single-grating monochromator.

Received: April 12, 1999
Final version: July 28, 1999

[1] S. Morita, A. A. Zakhidov, K. Yoshino, *Jpn. J. Appl. Phys.* **1993**, *32*, L873.
[2] N. S. Sariciftci, D. Braun, C. Zhang, V. I. Srdanov, A. J. Heeger, G. Stucky, F. Wudl, *Appl. Phys. Lett.* **1993**, *62*, 585.
[3] J. J. M. Halls, K. Pichler, R. H. Friend, S. C. Moratti, A. B. Holmes, *Appl. Phys. Lett.* **1996**, *68*, 3120.
[4] J. H. Burroughes, D. D. C. Bradley, A. R. Brown, R. N. Marks, K. Mackay, R. H. Friend, P. L. Burns, A. B. Holmes, *Nature* **1990**, *347*, 539.
[5] H. Koezuka, A. Tsumura, T. Ando, *Synth. Met.* **1987**, *18*, 699.
[6] R. N. Marks, J. J. M. Halls, D. D. C. Bradley, R. H. Friend, A. B. Holmes, *J. Phys.: Condens. Matter* **1994**, *6*, 1379.
[7] P. M. Ajayan, O. Stephan, C. Colliex, D. Trauth, *Science* **1994**, *265*, 1212.
[8] S. A. Curran, P. M. Ajayan, W. J. Blau, D. L. Carroll, J. N. Coleman, A. B. Dalton, A. P. Davey, A. Drury, B. McCarthy, S. Maier, A. Stevens, *Adv. Mater.* **1998**, *10*, 1091.
[9] D. B. Romero, M. Carrard, W. de Heer, L. Zuppiroli, *Adv. Mater.* **1996**, *8*, 899.
[10] H. Hiura, T. W. Ebbesen, K. Tanigaki, *Adv. Mater.* **1995**, *7*, 275.
[11] M. S. P. Shaffer, X. Fan, A. H. Windle, *Carbon* **1998**, *36*, 1603.
[12] J. S. Kim, M. Gransröm, R. H. Friend, N. Johansson, W. R. Salaneck, R. Daik, W. J. Feast, F. Cacialli, *J. Appl. Phys.* **1998**, *84*, 6859.
[13] H. Ago, M. S. P. Shaffer, D. S. Ginger, A. H. Windle, R. H. Friend, unpublished. The activation energy for the MWNT film was estimated to be 3–14 meV.
[14] A. B. Dalton, H. J. Byrne, J. N. Coleman, S. Curran, A. P. Davey, B. McCarthy, W. Blau, in *Proc. NANOTECH 98 (Nanotechnology in Carbon and Related Materials)*, Brighton, UK, Sept. 9–11, **1998**.
[15] F. Bommeli, L. Degiorgi, P. Wachter, W. S. Bacsa, W. A. de Heer, L. Forro, *Synth. Met.* **1997**, *86*, 2307.
[16] H. Ago, T. Kugler, F. Cacialli, W. R. Salaneck, M. S. P. Shaffer, A. H. Windle, R. H. Friend, *J. Phys. Chem. B*, in press.
[17] B. O'Regan, M. Grätzel, *Nature* **1991**, *353*, 737.
[18] J. J. M. Halls, C. A. Walsh, N. C. Greenham, E. A. Marseglia, R. H. Friend, S. C. Moratti, A. B. Holmes, *Nature* **1995**, *376*, 498.
[19] M. Granström, K. Petritsch, A. C. Arias, A. Lux, M. R. Andersson, R. H. Friend, *Nature* **1998**, *395*, 257.
[20] C. Niu, E. K. Sichel, R. Hoch, D. Moy, H. Tennet, *Appl. Phys. Lett.* **1997**, *70*, 1480.

## Patterned Films of Nanotubes Using Microcontact Printing of Catalysts**

By *Hannes Kind*,* *Jean-Marc Bonard*, *Christophe Emmenegger*, *Lars-Ola Nilsson*, *Klara Hernadi*, *Eliane Maillard-Schaller*, *Louis Schlapbach*, *László Forró*, and *Klaus Kern*

There is increasing experimental and theoretical evidence that carbon nanotubes[1] have remarkable physical

[*] H. Kind, Dr. J.-M. Bonard, Dr. L. Forró, Prof. K. Kern
Département de Physique,
École Polytechnique Fédérale de Lausanne
CH-1015 Lausanne (Switzerland)
C. Emmenegger, L.-O. Nilsson, Dr. E. Maillard-Schaller,
Prof. L. Schlapbach
Physics Department, University of Fribourg
Pérolles, CH-1700 Fribourg (Switzerland)
Dr. K. Hernadi
Applied Chemistry and Environment Department
Jozsef Attila University
H-6720 Szeged, Rerrich B. ter.1 (Hungary)
Prof. K. Kern
Max-Planck-Institut für Festkörperforschung
Heisenbergstrasse 1, D-70569 Stuttgart (Germany)

[**] We thank E. Delamarche, M. Geissler, H. Schmid, and B. Michel for providing us with masters and stamps and A. Bietsch and A. M. Bittner for helpful discussions. We are grateful to CIME-EPFL for access to SEM and TEM facilities. K. Hernadi thanks the National Science Foundation of Hungary for financial support (OTKA-T025246).

  0935-9648/99/1510-1285 $ 17.50+.50/0 

properties. Several interesting technological applications have been proposed during the last few years.[2–6] Among other important applications the use of carbon nanotubes as field-emission electron sources was proposed by de Heer[2] and others.[7,8] At a first glance, the idea of using carbon nanotubes as cold electron sources looks very promising. However, practical experience shows that several major problems have to be solved first before this will be possible.

One important prerequisite to using carbon nanotubes as electron emitters (e.g., for flat panel displays) is the need to apply them in a controlled way to the substrate in order to define pixels. It has been shown only recently that substrates can be patterned with carbon nanotubes using standard lithographic techniques.[9–11] Compared to such standard photolithographic techniques, soft lithography[12–14] is useful in several applications for which photolithography is not applicable or is very expensive, for example, patterning of large areas in one single process step or patterning of non-planar surfaces. One way to use soft lithography is microcontact printing (μCP): μCP uses a patterned and inked elastomeric stamp to print molecules or assemblies of molecules as a pattern onto substrates. Recently, inorganic solutions have been used as an ink to print catalysts on surfaces.[15,16] Substrates patterned with such catalysts in turn are able to induce chemical reactions that are inhibited at their bare surfaces (e.g., the electroless deposition of metals[15,16] or the decomposition of hydrocarbons for the growth of multiwalled carbon nanotubes). μCP of catalysts is a fast and easy one-step process with the advantage of not using any photoresist or costly machines such as evaporators and mask aligners. The choice of μCP to pattern silicon wafers allows one also to vary the density of the catalyst on the substrate by changing the concentration of the transition metal in the ink.

Another prerequisite to using carbon nanotubes as electron emitters is a profound understanding of the emission behavior of the nanotubes. Up to now, an increasing number of studies have addressed this aspect for single multiwalled nanotubes as well as for films of nanotubes (single-walled and multiwalled).[2,8,17–20] However, there are only very few studies of the emission properties of substrates patterned with multiwalled carbon nanotubes.[10,11] It is clear that a better understanding of the emission characteristics of patterned substrates is absolutely necessary for any technological application.

In the present communication we describe a simple but powerful way to use μCP to pattern silicon wafers with catalysts followed by the growth of multiwalled carbon nanotubes on the activated regions. The samples show patterns of high contrast and the pixels are covered by multiwalled carbon nanotubes about 10 nm in diameter and with well-graphitized walls. Preliminary results of the emission properties of such patterned samples are discussed.

Figure 1 outlines the fabrication of $SiO_2$/Si substrates[21] patterned with nanotubes. In the first step the poly(dimethylsiloxane) (PDMS) stamps[22] were hydrophilized[16,23] to considerably increase the affinity between the stamp surface and a variety of water- and ethanol-soluble catalysts. Stamps were subsequently inked or stored under water to prevent restructuring of the surface towards the hydrophobic-like state, which is stable in air. After drying the stamp, the catalyst was printed on the substrate. Samples were mounted in a tube reactor, where the deposition of carbon nanotubes was carried out using the catalytic decomposition of acetylene.[24,25]

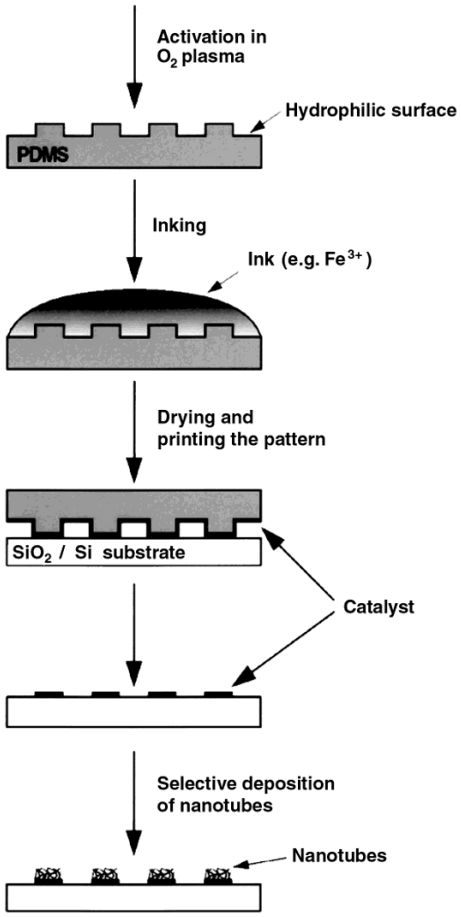


Fig. 1. Schematic representation of the microcontact printing process used for patterning carbon nanotubes onto $SiO_2$/Si wafers.

Transition metal catalysts such as Fe, Ni, and Co were explored earlier in an effort to control the size and morphology of the nanotubes, and to increase the yield compared to the deposition of other carbon allotropes. In this work several different pure and mixed catalysts ($Fe(NO_3)_3 \cdot 9H_2O$, $Ni(NO_3)_2 \cdot 6H_2O$, $Co(NO_3)_2 \cdot 6H_2O$, and mixtures of the preceding) were explored. It turned out that $Fe^{3+}$ is the only pure catalyst that can be printed in sufficient amounts and homogeneity over square centimeters onto silicon wafers. Printing the same concentrations of pure $Ni^{2+}$ or $Co^{2+}$ catalysts resulted in the formation of small crystallites of the catalysts on the stamp, which could be seen under the optical microscope. Such samples were not used for the deposition of carbon nanotubes. Mixtures

  0935-9648/99/1510-1286 $ 17.50+.50/0 

ADVANCED MATERIALS

of $Fe^{3+}$ with the two other metals resulted in deposits of good quality when the total concentration did not pass over 100 mM. Figures 2a–d show a typical pattern of nanotubes for a sample printed with a 100 mM $Fe^{3+}$ ethanolic solution. It is obvious that nanotubes can be patterned over large areas with a homogeneous density. The major requirement of selectivity of the printing step is fulfilled: the nanotubes are confined to the printed regions and completely absent between the structures. A slight broadening (~1–2 μm) of the structures occurred after the deposition as some nanotubes stand partially out of the structures. The proportion of nanotubes in the deposit is very high, reaching almost 100 %. Other carbon allotropes (e.g., amorphous carbon) are almost completely suppressed in the deposit.

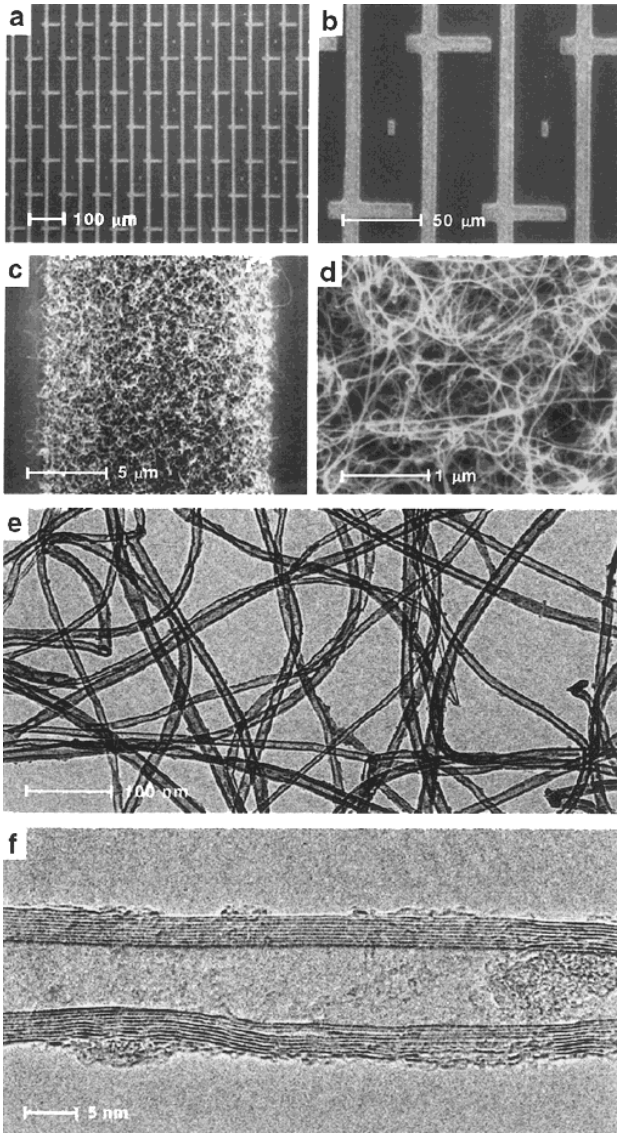


Fig. 2. Scanning electron microscopy images (a–d) of a surface with patterned carbon nanotubes at different scales and high-resolution transmission electron microscopy images (e,f) of the nanotubes. The substrate was prepared according to the procedures described in the experimental section with an ink concentration of 100 mM $Fe^{3+}$.

This is surprising since multiwalled carbon nanotubes produced by catalytic decomposition of hydrocarbons are usually accompanied by a large amount of amorphous carbon.[24,25] A possible explanation is that the major part of the catalyst is present in a chemically active state and shows a morphology (size and density of the catalytic particles) favoring the growth of multiwalled carbon nanotubes over the deposition of other carbon allotropes.[26]

High-resolution transmission electron microscopy (TEM) images (Figures 2e,f) again reveal the high yield and the structure of the multiwalled carbon nanotubes: well-graphitized walls, aligned with the tube axis, and some extended defects, which are typical for catalytic deposition. The average outer diameter varies between 8 and 20 nm and the walls are partially covered with amorphous carbon. Catalytic particles are sometimes found inside and at the end of the tubes as for the standard mass production of nanotubes by catalytic decomposition of carbon-containing gases. Varying the deposition temperature from 650 °C up to 850 °C and the flow of acetylene gas from 2 mL/min to 40 mL/min did not change the quality of the multiwalled carbon nanotubes significantly.

To evaluate the possibility of tuning the density of the carbon nanotubes in the printed zones we varied the concentration of the catalyst in the ink. Decreasing the ink concentration from 100 to 10 and 1 mM $Fe^{3+}$ was followed by a similar decrease in the density of the nanotubes. For the latter concentration only a few single nanotubes were found on the printed structures. However, a change in the morphology of the nanotubes was not detected by TEM measurements. Increasing the ink concentration to about 120 mM $Fe^{3+}$ resulted in the structures shown in Figure 3. At such high concentrations nanotubes can form "brushes" standing perpendicular to the surface. Each block exhibits flat side walls and only very few tubes are branching away. The widths of the blocks are the same as that of the printed pattern. High-magnification scanning electron microscopy (SEM) images (Fig. 3b–d) show that some nanotubes stand out above the top of the block and that the tubes within a block are more or less parallel to each other. For growth times of 30 min in a flow of acetylene, the height of the brushes varied in the range 5–15 μm on the same sample. The reason why these inhomogeneities in height occur is still not clear and further experiments to clarify this issue are in progress. Increasing the ink concentration above 150 mM results in deposits of almost only amorphous carbon. Considering the temperatures used in our experiments it is clear that catalytic particles can migrate on the surface and form bigger aggregates.[26,27] For these very high ink concentrations the aggregates grow too large and only amorphous carbon is deposited on the catalytic pattern since the growth of carbon nanotubes requires a well-defined size of the catalytic particles.[28] X-ray photoelectron spectroscopy (XPS) measurements showed that (for all ink concentrations used) the catalyst is present in the $Fe^{3+}$ state when the decomposition of acetylene starts. This gives us a

  0935-9648/99/1510-1287 $ 17.50+.50/0 

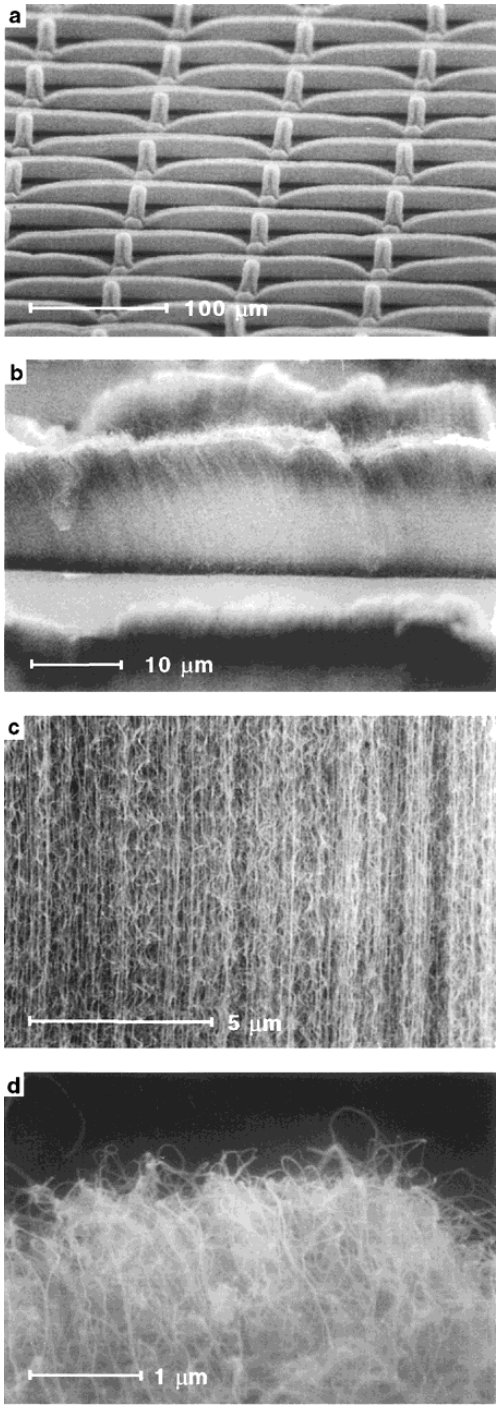


Fig. 3. Scanning electron microscopy images of a surface patterned with carbon nanotubes. For the printing process a concentrated ink (120 mM $Fe^{3+}$) was used. The carbon nanotubes were deposited according to the standard deposition procedure. To show that the nanotubes stand perpendicular to the substrate the e-beam was used at 45° incidence.

further indication that in our case the parameters for a high-quality deposit of nanotubes are indeed the density and the size of the catalytic particles.

The morphology of the nanotube patterns can be an extremely important factor influencing the emission behavior of the samples. To examine this we performed a series of preliminary experiments in an emission chamber: a constant voltage was applied to a tip scanning at constant height over the sample and the resulting field emission current was measured. Measurements were performed on samples printed with 1, 10, and 100 mM $Fe^{3+}$ followed by the standard deposition routine at 750 °C. The emission images reproduce the printed pattern. Linewidths are broadened because the current image is a convolution of tip apex, tip–sample distance, and the morphology of the deposited patterns. A clear contrast between the emitting structures of multiwalled carbon nanotubes and the bare substrate is visible and proves the selectivity of the printing and in turn the ability of the nanotubes to emit electrons. However, the current intensity within the features is found to be not very homogeneous. This is due to the fact that very small differences (e.g., slight differences in height, in the density of the nanotubes, or in their diameters) of the deposit significantly change the emission properties of the samples. To ensure that there is no contribution to the emission current from the catalytic particles a pattern of catalyst without any carbon deposition was examined. Scans acquired with the same field applied between tip and sample did not show any emission. This proves that the carbon nanotubes act as the emitters and not the catalytic particles. Finally, we would like to emphasize that our samples show macroscopic emission performances that are comparable to arc-discharge multiwalled nanotube film emitters although only 10 % of the surface is patterned with nanotubes in our case.[20]

The goal of this work was to show that microcontact printing (μCP) is a promising tool for patterning silicon wafers with catalysts and, in turn, for patterning the surface with multiwalled carbon nanotubes. In addition, first preliminary results performed with a new emission scanner proved the selectivity and quality of μCP and gave a first—more macroscopic and collective—insight into the emission properties of nanotube assemblies constrained to certain geometric patterns. In the future a better understanding of the behavior of the catalyst in the ink, during the printing step, and on the substrate should help to produce homogeneous arrays of nanotubes standing perpendicular to the substrate.

## *Experimental*

*Stamps and Substrates*: Patterned poly(dimethylsiloxane) stamps were prepared from Sylgard 184 (Dow Corning, Midland MI) and cured for at least 12 h at 60 °C on masters prepared by UV-lithography and fluorinated with a monolayer of (1,1,2,2,-tetrahydroperfluorodecyl)-trichlorosilane [22]. Stamps had a thickness of ~4–5 mm. We used an $O_2$ plasma treatment of the stamps (oxygen pressure ~0.8 torr, load coil power ~75 W, 60 s) to render their surface hydrophilic prior to inking. Hydrophylized stamps were used immediately or stored under water. $SiO_2$/Si wafers were used as received.

*Inking and Printing*: Wet inking involved placing a drop of a 1–500 mM $Fe(NO_3)_3{\cdot}9H_2O$ (or 50:50 $Fe(NO_3)_3{\cdot}9H_2O$ and $Ni(NO_3)_2{\cdot}6H_2O$ or $Co(NO_3)_2{\cdot}6H_2O$) ethanolic solution onto the patterned stamp for 15 s (the freshly prepared ink was used within 6 h). The stamp was then dried for 10 s under a continuous stream of $N_2$. Inked stamps were used to print within ~15 s after their inking. Printing wet-inked stamps was done by placing the stamps on substrates and removing them by hand. The time of conformal

  0935-9648/99/1510-1288 $ 17.50+.50/0 

ADVANCED MATERIALS

contact between stamp and substrate was 3 s. For each print we used a newly patterned stamp to prevent interference from the history of the stamp with the next print.

*Deposition of Multiwalled Carbon Nanotubes*: The deposition of multiwalled carbon nanotubes was carried out in a tube reactor (quartz tube of 14 mm diameter in a horizontal oven) at a reaction temperature of typically 750 °C. The samples were mounted in the tube reactor and the system was purged with 80 mL/min nitrogen for 10 min before a mixture of 15 mL/min acetylene and 75 mL/min nitrogen was introduced at atmospheric pressure for 30 min. Finally the system was purged again with 80 mL/min nitrogen for 10 min.

*Instrumentation*: The nanotube deposits were examined using a Jeol 6300 F scanning electron microscope (SEM) operated at 5 kV. High-resolution transmission (TEM) electron micrographs were taken with a Philips CM 300 microscope operated at 300 kV. For the emission experiments a scanning system was mounted in a vacuum chamber working at a pressure of ~$5 \times 10^{-7}$ mbar. A tip with a radius of 2–5 μm was scanned over the surfaces with an *xy* stepping motor at a constant height typically 3–6 μm above the surface. The voltage was held constant and the current was measured every 3 μm with a Keithley 237.

Received: April 26, 1999


[1] S. Iijima, *Nature* **1991**, *354*, 56.
[2] W. A. de Heer, A. Châtelain, D. Ugarte, *Science* **1995**, *270*, 1179.
[3] Q. H. Wang, T. D. Corrigan, J. Y. Dai, R. P. H. Chang, A. R. Krauss, *Appl. Phys. Lett.* **1997**, *24*, 3308.
[4] *Carbon Nanotubes: Preparation and Properties* (Ed: T. W. Ebbesen), CRC Press, Boca Raton, FL **1997**.
[5] S. S. Wong, E. J. Joselevich, A. T. Woolley, C. L. Cheung, C. M. Lieber, *Nature* **1998**, *394*, 52.
[6] Z. F. Ren, Z. P. Huang, J. W. Xu, J. H. Wang, P. Bush, M. P. Siegal, P. N. Provencio, *Science* **1998**, *282*, 1105.
[7] G. Che, B. B. Lakshmi, E. R. Fisher, C. R. Martin, *Nature* **1998**, *393*, 346.
[8] J.-M. Bonard, J. P. Salvetat, T. Stöckli, W. A. de Heer, L. Forró, A. Châtelain, *Appl. Phys. Lett.* **1998**, *73*, 918.
[9] J. Kong, H. T. Soh, A. M. Cassell, C. F. Quate, H. Dai, *Nature* **1998**, *395*, 878.
[10] Q. H. Wang, A. A. Setlur, J. M. Lauerhaas, J. Y. Dai, E. W. Selig, R. P. H. Chang, *Appl. Phys. Lett.* **1998**, *72*, 2912.
[11] S. Fan, M. G. Chapline, N. R. Franklin, T. W. Tombler, A. M. Cassell, H. Dai, *Science* **1999**, *283*, 512.
[12] A. Kumar, G. M. Whitesides, *Appl. Phys. Lett.* **1993**, *63*, 2002.
[13] Y. Xia, G. M. Whitesides, *Angew. Chem. Int. Ed.* **1998**, *37*, 550.
[14] H. A. Biebuyck, N. B. Larsen, E. Delamarche, B. Michel, *IBM J. Res. Dev.* **1997**, *41*, 159.
[15] P. C. Hidber, W. Helbig, E. Kim, G. M. Whitesides, *Langmuir* **1996**, *12*, 1375.
[16] H. Kind, M. Geissler, H. A. Biebuyck, H. Schmid, B. Michel, K. Kern, E. Delamarche, in preparation.
[17] P. G. Collins, A. Zettl, *Appl. Phys. Lett.* **1996**, *69*, 1969.
[18] Y. Saito, K. Hamaguchi, K. Hata, K. Tohji, A. Kasuya, Y. Nishina, K. Uchida, Y. Tasaka, F. Ikazaki, M. Yumura, *Ultramicroscopy* **1998**, *73*, 1.
[19] O. M. Küttel, O. Gröning, C. Emmenegger, L. Schlapbach, *Appl. Phys. Lett.* **1998**, *73*, 2113.
[20] J.-M. Bonard, J. P. Salvetat, T. Stöckli, L. Forro, A. Châtelain, *Appl. Phys. A*, in press.
[21] Nanoporous $SiO_2$/Si substrates were used in addition to $SiO_2$/Si substrates. Patterned deposits on these samples showed lower densities of nanotubes and blurred edges. This is probably due to a decreased conformal contact between the stamp and the substrate.
[22] E. Delamarche, H. Schmid, B. Michel, H. A. Biebuyck, *Adv. Mater.* **1997**, *9*, 741.
[23] M. K. Chaudhury, G. M. Whitesides, *Langmuir* **1991**, *7*, 1013.
[24] K. Hernadi, A. Fonseca, P. Piedigrosso, M. Delvaux, J. B. Nagy, D. Bernaerts, J. Riga, *Catal. Lett.* **1997**, *48*, 229.
[25] H. Dai, A. G. Rinzler, P. Nikolaev, A. Thess, D. T. Colbert, R. E. Smalley, *Chem. Phys. Lett.* **1996**, *260*, 471.
[26] Changing the pH of the ink solution by adding $NH_3$ did not change the activity of the catalysts significantly. More results about the chemical state and morphology of the catalyst and its influence on the morphology of the deposit and the emission properties of the nanotubes will be reported in a forthcoming publication.
[27] P. Mauron, personal communication.
[28] M. Yudasaka, R. Kikuchi, Y. Okhi, E. Ota, S. Yoshimura, *Appl. Phys. A* **1997**, *70*, 1817.


## New Method for Nanofabrication of Structures Analogous to "Core–Shell" Vesicles**

By *Oleg Palchik*,* *Gina Kataby*, *Yitzhak Mastai*, and *Aharon Gedanken*

The preparation and characterization of nanostructure materials is an active field in materials science, due to their interesting properties.[1,2] The general trend is not only to prepare simple nanophase materials, but also to design and to arrange them in complex functional structures.[3] This advanced approach requires new methods of formation of nanoparticles with subsequent organization into complex systems. The most promising approach to organization is self-assembly.[4] In living organisms the self-assembly method is used for routine and accurate production of complex, spatially well-defined, and functional mesoscopic structures, such as lipids and polypeptide vesicles.[5–7] There are a few examples in the literature of so-called core–shell nanoparticles.[8] The chemical nature of the core and shell could be different, as is the case with hybrids, which have an inorganic core and an organic shell.[9] The widespread organic shells are composed of different surfactant molecules, which are self-assembled on the surface of an inorganic core. Generally, the formation of core–shell vesicles occurs in two steps: formation of the inorganic core with subsequent generation of the shell, or formation of an empty vesicle, which plays the role of a microreactor for crystallization of the inorganic core.[10] In this study we find that ultrasound irradiation is an excellent method for the simultaneous (one-step) synthesis of structures analogous to "core–shell" vesicles, in which the core is an inorganic compound, and the shell is an organo-silicon polymer.

Recently there has been a rapid increase in the application of unconventional methods to chemistry. Sonochemistry[11] is one of these unusual methods. It is based on acoustic cavitation,[12,13] that is, the formation, growth and collapse of bubbles in a liquid. The implosive collapse of bubbles generates localized hot spots with transient temperatures of ~5000 K, pressures ~1800 atm, and cooling rates in excess of 1010 K/s. Due to fast cooling rates during sonication, numerous examples exist in which the product is formed in the amorphous phase.[13,14] Using this technique we have explored several syntheses of nanostructured[15–17] inorganic materials. This is the first report of

[*] Dr. O. Palchik, Dr. G. Kataby, Prof. A. Gedanken
Department of Chemistry
Bar-Ilan University
52900 Ramat-Gan (Israel)
Dr. Y. Mastai
Department of Materials and Interfaces
Weizmann Institute of Science
76100 Rehovot (Israel)

[**] This project was financially supported by a NEDO International Joint Research Grant, and by the German Ministry of Education and Research through the Deutsch-Israeli Program DIP.

  0935-9648/99/1510-1289 $ 17.50+.50/0 